© 2012 Society for Industrial and Applied Mathematics

MIXED FINITE ELEMENT METHOD FOR A DEGENERATE CONVEX VARIATIONAL PROBLEM FROM TOPOLOGY OPTIMIZATION[*]

CARSTEN CARSTENSEN[†], DAVID GÜNTHER[‡], AND HELLA RABUS[§]

Abstract. The optimal design task of this paper seeks the distribution of two materials of prescribed amounts for maximal torsion stiffness of an infinite bar of a given cross section. This example of relaxation in topology optimization leads to a degenerate convex minimization problem $E(v) := \int_\Omega \varphi_0(|\nabla v|)\, dx - \int_\Omega fv\, dx$ for $v \in V := H_0^1(\Omega)$ with possibly multiple primal solutions u, but with unique stress $\sigma := \varphi_0'(|\nabla u|)\operatorname{sign}\nabla u$. The mixed finite element method is motivated by the smoothness of the stress variable $\sigma \in H_{\mathrm{loc}}^1(\Omega; \mathbb{R}^2)$, while the primal variables are uncontrollable and possibly nonunique. The corresponding nonlinear mixed finite element method is introduced, analyzed, and implemented. The striking result of this paper is a sharp a posteriori error estimation in the dual formulation, while the a posteriori error analysis in the primal problem suffers from the reliability-efficiency gap. An empirical comparison of that primal formulation with the new mixed discretization schemes is intended for uniform and adaptive mesh refinements.

Key words. adaptive finite element method, adaptive mixed finite element method, optimal design, degenerate convex minimization

AMS subject classifications. 65K10, 65N30

DOI. 10.1137/100806837

1. Introduction. This paper appears to be the first attempt to utilize mixed finite element methods (MFEMs) for degenerate minimization problems in the calculus of variations. The usage of MFEMs [5] in relaxed formulations for macroscopic simulations in computational microstructures [3, 7, 9, 24] is motivated by the properties of the primal and dual variables. The primal variables (e.g., a deformation or displacement) may be nonunique [17] or less regular, while the dual (e.g., a flux or stress) variable is unique and locally smooth [6]. Hence a mixed scheme, which relies on smooth dual variables, might enjoy superior convergence properties.

The model problem is motivated by an optimal design problem, where a given domain $\Omega \subset \mathbb{R}^2$ has to be filled with two materials of different elastic shear stiffnesses with energy

$$(1.1) \qquad E(v) := \int_\Omega \varphi_0(|\nabla v|)\, dx - \int_\Omega fv\, dx \quad \text{for } v \in V := H_0^1(\Omega)$$

for a given right-hand side $f \in L^2(\Omega)$ and the energy density function $\varphi_0 \in C^0([0, \infty); \mathbb{R})$ of section 2.

The model has been analyzed in [18, 11, 22, 23] and computed in [19, 20, 21, 6]. Recently, a convergent adaptive finite element method in its primal form was introduced in [4].

While the solutions of the primal and dual problem coincide in the continuous case, this does not need to be true for discrete calculations in general. In the dual formulation, we avoid the difficulties arising from the fact that the gradient of the energy density functional φ_0' is not strongly monotone. This may lead to multiple primal variables u, while there is a unique stress-type variable $\sigma := \varphi_0'(|\nabla u|)\operatorname{sign}\nabla u$ [6, 8, 4]. In contrast to the continuous differentiability of φ_0', its conjugate function φ_0^* is solely Lipschitz continuous. To overcome the lack of differentiability we approximate φ_0^* by its Yosida regularization φ_ε^*.

The proposed mixed formulation is based on the following dual formulation: Seek $(u, \sigma) \in L^2(\Omega) \times H(\operatorname{div}, \Omega)$ with

$$(\mathbf{D}) \qquad\qquad \operatorname{div}\sigma + f = 0 \quad \text{and} \quad \nabla u \in \partial \Phi_0^*(\sigma) \quad \text{in } \Omega.$$

The discretization is based on piecewise polynomial subspaces $RT_0(\mathcal{T}) \subseteq H(\operatorname{div}, \Omega)$ and $\mathcal{P}_0(\mathcal{T}) \subseteq L^2(\Omega)$ named after Raviart and Thomas and introduced in section 3. For $\varepsilon > 0$ piecewise constant with respect to $\mathcal{T}$, the discrete regularized dual problem reads as follows: Seek $(u_{\varepsilon h}, \sigma_{\varepsilon h}) \in \mathcal{P}_k(\mathcal{T}) \times RT_k(\mathcal{T})$ such that for all $(v_h, \tau_h) \in \mathcal{P}_k(\mathcal{T}) \times RT_k(\mathcal{T})$ it holds that

$$(\mathbf{D}_{\varepsilon h}) \qquad \begin{aligned} (\tau_h, \mathrm{D}\Phi_\varepsilon^*(\sigma_{\varepsilon h}))_{L^2(\Omega)} + (u_{\varepsilon h}, \operatorname{div}\tau_h)_{L^2(\Omega)} &= 0, \\ (v_h, \operatorname{div}\sigma_{\varepsilon h})_{L^2(\Omega)} + (f, v_h)_{L^2(\Omega)} &= 0. \end{aligned}$$

The main theorems in section 3 verify that poor a priori error estimates are caused by the lack of smoothness, while efficient and reliable a posteriori error estimates are derived. Numerical simulations show that the convergence of the adaptive scheme is improved in the presence of geometric singularities such as nonconvex corners. Furthermore, compared to the primal formulation as considered in [4], the experiments of section 6 of the regularized dual mixed form reveal reduced convergence rates but no efficiency-reliability gap.

The remaining parts of the paper are organized as follows. Section 2 covers a preliminary analysis of the model problem and its energy density function. The regularized and discrete mixed formulation of the problem is introduced in section 3, followed by the investigation of the existence and uniqueness of the exact and discrete solutions in section 4. Section 5 presents a thorough a priori and a posteriori error analysis. The adaptive mesh-refining algorithm and some numerical experiments conclude the paper in section 6.

In this paper we follow the standard notation for the Lebesgue $L^2(\Omega)$, $L^2(\Omega; \mathbb{R}^2)$ and Sobolev $H^1(\Omega)$, $H^1(\Omega; \mathbb{R}^2)$ spaces; $H(\operatorname{div}, \Omega)$ denotes the Hilbert space of L^2-functions with square-integrable divergence. The $L^2(\Omega)$ scalar product is abbreviated by $(.,.)_{L^2(\Omega)}$, while $\langle \cdot, \cdot \rangle$ denotes the scalar product in $\mathbb{R}^n$.

2. Preliminaries.

2.1. An optimal design problem. The task is to seek the distribution of two materials of a fixed volume fraction in the cross section of an infinite bar given by the domain $\Omega \subseteq \mathbb{R}^2$ for maximal torsion stiffness. The focus of this paper lies on the analysis and numerical studies of the variational problem, while the precise mathematical modeling may divert from the emphasis of this paper. For details on the mathematical modeling the reader is referred to [4, section 2] and the references given in section 1.

Let $0 < t_1 < t_2$ and the reciprocal shear stiffness $0 < \mu_1 < \mu_2 < \infty$ with $t_1\mu_2 = \mu_1 t_2$, and let $0 < \xi < 1$ represent the ratio of amounts of the two materials, $|\Omega_1| = \xi\,|\Omega|$, $|\Omega_2| = \Omega - |\Omega_1|$, and $t_1 = \sqrt{2\lambda\mu_1/\mu_2}$. The Lagrange parameter $\lambda \in \mathbb{R}$ is fixed for a specific geometry Ω and the choice of ξ [4, 14, 17, 18, 19, 20, 21].

In the relaxed formulation of the model from [19, 20, 21], the right-hand side $f \equiv 1$ is constant and the locally Lipschitz continuous energy density function $\varphi_0 : [0,\infty) \to \mathbb{R}$ reads as

$$\varphi_0(t) = \lambda\xi(\mu_1 - \mu_2) + \begin{cases} \frac{\mu_2}{2}t^2 & \text{for } 0 \leq t \leq t_1, \\ t_1\mu_2\left(t - \frac{t_1}{2}\right) & \text{for } t_1 \leq t \leq t_2, \\ \frac{\mu_1}{2}t^2 + \frac{\mu_1 t_2}{2}(t_2 - t_1) & \text{for } t_2 \leq t. \end{cases}$$

Thus, the primal formulation is the minimization of E in (1.1). There exist minimizers of E which are not necessarily unique. For $f \in L^2(\Omega)$, the stress field $\sigma := \varphi_0'(|\nabla u|)\operatorname{sign}\nabla u$ is unique and locally smooth, i.e., $\sigma \in H^1_{\mathrm{loc}}(\Omega;\mathbb{R}^2)$, while $f \in H^1_0(\Omega)$ (excluded in this work) implies $\sigma \in H^1(\Omega,\mathbb{R}^2)$; cf. [6].

2.2. Dual functional and Yosida regularization. Direct calculations lead to the dual function φ_0^* of φ_0 and its Yosida regularization φ_ε^* as stated in the following lemma. We use the standard notation of convex analysis [25].

LEMMA 2.1. *The dual (or conjugate) function φ_0^* of φ_0 reads as*

$$\varphi_0^*(t) = -\lambda\xi(\mu_1 - \mu_2) + \begin{cases} \frac{t^2}{2\mu_2} & \text{for } t \leq t_1\mu_2, \\ \frac{t^2}{2\mu_1} - \frac{\mu_1 t_2^2}{2} + \frac{t_1^2\mu_2}{2} & \text{for } t_1\mu_2 \leq t. \end{cases}$$

It is piecewise polynomial and globally convex, and it is Lipschitz continuous on compact subsets but not differentiable at $t = t_1\mu_2 = \mu_1 t_2$.

For fixed $\varepsilon > 0$ and all $t \geq 0$, the Yosida regularization φ_ε^* of φ_0^* is defined by $\varphi_\varepsilon^*(t) := \inf_{z\in\mathbb{R}}(\varphi^*(z) + \frac{1}{2\varepsilon}|t - z|^2)$ and equals

$$\varphi_\varepsilon^*(t) = -\lambda\xi(\mu_1 - \mu_2) + \begin{cases} \frac{t^2}{2(\varepsilon+\mu_2)} & \text{for } 0 \leq t < t_1(\varepsilon + \mu_2), \\ \frac{\mu_2}{2}t_1^2 + \frac{1}{2\varepsilon}|t_1\mu_2 - t|^2 & \text{for } t_1\mu_2 + \varepsilon t_1 \leq t \leq t_1\mu_2 + \varepsilon t_2, \\ \frac{t^2}{2(\mu_1+\varepsilon)} - \frac{\mu_1 t_2^2}{2} + \frac{t_1^2\mu_2}{2} & \text{for } t_2(\mu_1 + \varepsilon) < t. \end{cases}$$

Let $C_\mu := \frac{1}{\mu_1^2} + \frac{1}{2\mu_2^2}$. *Then, the difference of φ_0^* and φ_ε^* is bounded in the sense that*

$$0 \leq \sup_{z\in\mathbb{R}}\left(\varphi_0^*(t) - \varphi_0^*(z) - \frac{1}{2\varepsilon}|t - z|^2\right) = \varphi_0^*(t) - \varphi_\varepsilon^*(t) \leq C_\mu\varepsilon t^2 \leq \mathcal{O}(\varepsilon)t^2. \qquad \square$$

The function φ_ε^* is differentiable, and hence the subgradient $\partial\varphi_\varepsilon^*(a) = \{(\varphi_\varepsilon^*)'(a)\}$ is a singleton, while φ_0^* is not smooth and $\partial\varphi_0^*(t_1\mu_2) = [t_1, t_2]$ is a compact interval. The differentials φ_0', $\partial\varphi_\varepsilon^*$, and $(\varphi_\varepsilon^*)'$ are depicted in the following sketch.

2.3. Remarks on φ_ε, φ_ε^* and Φ_ε, Φ_ε^*.
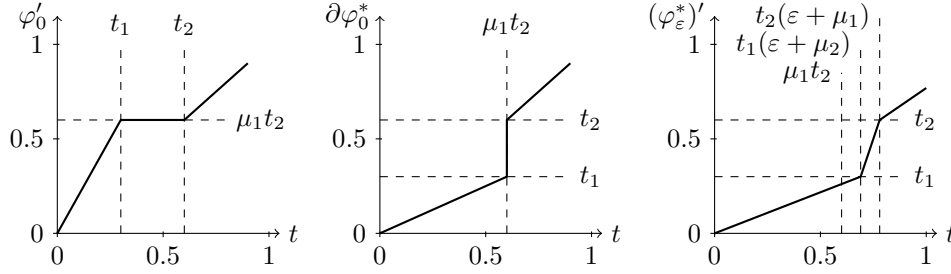
The energy density function

$$\Phi_\varepsilon : \mathbb{R}^n \to \mathbb{R}, \quad \Phi_\varepsilon(F) := \varphi_\varepsilon(|F|) \quad \text{for all } F \in \mathbb{R}^n,$$

its dual, and its regularized dual function enjoy the following properties.

(i) *Φ_ε and Φ_ε^*.* For any $\varepsilon > 0$ the function $\Phi_\varepsilon := \varphi_\varepsilon(|\cdot|)$ satisfies

$$\mathrm{D}\Phi_\varepsilon(F) = \varphi_\varepsilon'(|F|)\,\mathrm{sign}\,F \quad \text{for all } F \in \mathbb{R}^n$$

with the unit ball $B(0,1) := \{x \in \mathbb{R}^n \mid |x| \le 1\}$ and

$$\mathrm{sign}\,F := \begin{cases} B(0,1) & \text{if } |F| = 0, \\ F/|F| & \text{otherwise.} \end{cases}$$

Notice that $\varphi_\varepsilon'(0) = 0$ and $\varphi_\varepsilon(0) = \varphi_0(0) = 0$ imply

$$\mathrm{D}\Phi_\varepsilon(F) = \begin{cases} \varphi_\varepsilon'(|F|)F/|F| & \text{if } |F| \ne 0, \\ 0 & \text{otherwise.} \end{cases}$$

For $\varepsilon > 0$ and all $F \in \mathbb{R}^n$, the dual of $\Phi_\varepsilon = \varphi_\varepsilon(|\cdot|)$ reads as

$$\Phi_\varepsilon^*(F) = \varphi_\varepsilon^*(|F|) \text{ for all } F \in \mathbb{R}^n$$

and

$$\mathrm{D}\Phi_\varepsilon^*(F) = (\varphi_\varepsilon^*)'(|F|)\,\mathrm{sign}\,F.$$

For $\varepsilon = 0$, $\Phi_0^* := \varphi_0^*(|\cdot|)$ satisfies

$$\partial\Phi_0^*(F) = \partial\varphi_0^*(|F|)\,\mathrm{sign}\,F \quad \text{for all } F \in \mathbb{R}^n.$$

(ii) *Convexity control for Φ_0.* The function Φ_0 allows convexity control in the sense that for all $a, b \in \mathbb{R}^n$, $A \in \partial\Phi_0(a)$, and for all $B \in \partial\Phi_0(b)$, it holds that

$$\frac{1}{\mu_2}|A - B|^2 \le \langle A - B, a - b\rangle.$$

(iii) *Strong monotonicity of $\partial\Phi_\varepsilon^*$.* The subgradient $\partial\Phi_\varepsilon^*$ is strongly monotone in the sense that, with $C_M := \mu_2 + \varepsilon$ and $\varepsilon \ge 0$, it holds that

$$\mu_2|a - b|^2 \le C_M|a - b|^2 \le \langle \partial\Phi_\varepsilon^*(a) - \partial\Phi_\varepsilon^*(b), a - b\rangle \quad \text{for all } a, b \in \mathbb{R}^n.$$

(iv) *Strong convexity of Φ_ε^**. For all $\varepsilon \geq 0$, the strong monotonicity of $\partial \Phi_\varepsilon^*$ and the definition of the subdifferential lead to

$$2\mu_2 \left| a - b \right|^2 \leq 2C_{\mathrm{M}} \left| a - b \right|^2 \leq \langle \partial \Phi_\varepsilon^* (a), a - b \rangle - \Phi_\varepsilon^* (a) + \Phi_\varepsilon^* (b)$$

for all $a, b \in \mathbb{R}^n$; cf. [16, Thm. D2.6.1]. Hence, Φ_ε^*; is strongly convex.

(v) *Lipschitz continuity of $(\varphi_\varepsilon^*)'$*. For all $\varepsilon > 0$, φ_ε^* is continuously differentiable and

$$(\varphi_\varepsilon^*)'(t) = \begin{cases} \frac{t}{\mu_2 + \varepsilon} & \text{for } t < t_1(\mu_2 + \varepsilon), \\ \frac{t - t_1 \mu_2}{\varepsilon} & \text{for } t_1 \mu_2 + \varepsilon t_1 \leq t \leq t_1 \mu_2 + \varepsilon t_2, \\ \frac{t}{\mu_1 + \varepsilon} & \text{for } t_2(\mu_1 + \varepsilon) < t \end{cases}$$

is Lipschitz continuous with Lipschitz constant $\mathrm{Lip}(\mathrm{D}\varphi_\varepsilon^*) = 1/\varepsilon$.

(vi) *Discontinuity of $\partial \Phi_0^*$*. The subgradient $\partial \Phi_0^*$ is piecewise Lipschitz continuous and jumps at $|z| = \mu_1 t_2$. However, the following estimate holds:

$$\left| \partial \Phi_0^* (a) - \partial \Phi_0^* (b) \right| \leq \delta (a, b) + \left| a - b \right| / \mu_1$$

for all $a, b \in \mathbb{R}^n$ with

$$\delta (a, b) := \begin{cases} t_2 - t_1 & \text{if } \min \{ |a|, |b| \} \leq t_1 \mu_2 \leq \max \{ |a|, |b| \}, \\ 0 & \text{otherwise.} \end{cases}$$

This estimate can be extended to Φ_ε^* and $\varepsilon \geq 0$ in the sense that

$$\left| \partial \Phi_\varepsilon^* (a) - \partial \Phi_\varepsilon^* (b) \right| \leq \delta_\varepsilon(a, b) + \left| a - b \right| / (\mu_1 + \varepsilon)$$
$$\leq \delta_\varepsilon(a, b) + \left| a - b \right| / \mu_1$$

for all $a, b \in \mathbb{R}^n$ with

$$\delta_\varepsilon (a, b) := \begin{cases} t_2 - t_1 & \begin{array}{l} \text{if } \exists t \in t_1 \mu_2 + \varepsilon[t_1, t_2] \text{ such that} \\ \quad \min \{ |a|, |b| \} \leq t \leq \max \{ |a|, |b| \}, \end{array} \\ 0 & \text{otherwise.} \end{cases}$$

3. Mixed formulation and its discretizations.

3.1. Motivation for mixed formulation. The direct method of calculus of variations yields the existence of a minimizer u of E in $V := H_0^1 (\Omega)$ with

(3.1)
$$E(v) := \int_\Omega (\varphi_0 (|\nabla v|) - fv) \, \mathrm{dx}.$$

The exact stress $\sigma = \varphi_0' (|\nabla u|) \operatorname{sign} (\nabla u)$ satisfies the equilibrium $\operatorname{div} \sigma + f = 0$ in Ω as the strong form of the Euler–Lagrange equations. Given any right-hand side $f \in L^2(\Omega)$ and the convex C^1-functional $\Phi_0 : \mathbb{R}^n \to \mathbb{R}$, the pair $(u, \sigma) \in V \times H(\operatorname{div}, \Omega)$ solves the primal mixed formulation

(**P**)
$$\operatorname{div} \sigma + f = 0 \quad \text{and} \quad \sigma = \mathrm{D}\Phi_0 (\nabla u) \quad \text{in } \Omega.$$

By duality of convex functions it holds, for all $\alpha, a \in \mathbb{R}^n$, that

$$\alpha \in \partial \Phi_0(a) \Leftrightarrow a \in \partial \Phi_0^*(\alpha).$$

This allows the reformulation

$$\sigma = D\Phi_0(\nabla u) \Leftrightarrow \nabla u \in \partial \Phi_0^*(\sigma).$$

Consequently, (**P**) reads in terms of the conjugated functional as

(**D**) $$\operatorname{div}\sigma + f = 0 \quad \text{and} \quad \nabla u \in \partial \Phi_0^*(\sigma) \quad \text{in } \Omega.$$

3.2. Regularized mixed formulation. For a C^1-regularization φ_ε^* of φ_0^* with $\varphi_\varepsilon^* \longrightarrow \varphi_0^*$ as $\varepsilon \to 0$, the regularized problem of (**D**) reads as follows: Given any $\varepsilon > 0$ piecewise constant on $\mathcal{T}$, seek $(u_\varepsilon, \sigma_\varepsilon) \in V \times H(\operatorname{div}, \Omega)$ with

$$\operatorname{div}\sigma_\varepsilon + f = 0 \quad \text{and} \quad \nabla u_\varepsilon = D\Phi_\varepsilon^*(\sigma_\varepsilon) \quad \text{in } \Omega.$$

The corresponding weak mixed formulation (**D**$_\varepsilon$) reads as follows: Seek $(u_\varepsilon, \sigma_\varepsilon) \in L^2(\Omega) \times H(\operatorname{div}, \Omega)$ such that for all $(v, \tau) \in L^2(\Omega) \times H(\operatorname{div}, \Omega)$ it holds that

(**D**$_\varepsilon$)
$$(\tau, D\Phi_\varepsilon^*(\sigma_\varepsilon))_{L^2(\Omega)} + (u_\varepsilon, \operatorname{div}\tau)_{L^2(\Omega)} = 0,$$
$$(v, \operatorname{div}\sigma_\varepsilon)_{L^2(\Omega)} + (f, v)_{L^2(\Omega)} = 0.$$

3.3. Discrete formulation. Given a shape-regular triangulation $\mathcal{T}$ into triangles T of Ω which covers $\bar{\Omega} = \cup_{T \in \mathcal{T}} T$ exactly, let $\mathcal{E}$ denote the set of edges E of $\mathcal{T}$ and $\mathcal{E}(\Omega)$ the set of interior edges. For any $k = 0, 1, 2, \ldots$, set

$$\mathcal{P}_k(T) := \{\text{polynomials on } T \text{ of total degree } \leq k\},$$
$$\mathcal{P}_k(\mathcal{T}) := \left\{v \in L^2(\Omega) \mid v|_T \in \mathcal{P}_k(T) \text{ for all } T \in \mathcal{T}\right\},$$
$$\mathcal{S}_k(\mathcal{T}) := \left\{v \in \mathcal{P}_k(\mathcal{T}) \mid v \text{ globally continuous in } \bar{\Omega}\right\},$$
$$\mathcal{S}_{k,0}(\mathcal{T}) := \{v \in \mathcal{S}_k(\mathcal{T}) \mid v = 0 \text{ on } \partial\Omega\},$$
$$RT_k(T) := \left\{(x, y) \mapsto \begin{pmatrix} p_1(x, y) \\ p_2(x, y) \end{pmatrix} + p_3(x, y)\begin{pmatrix} x \\ y \end{pmatrix} \middle| p_1, p_2, p_3 \in \mathcal{P}_k(T)\right\}.$$

Let $[p]_E := p|_{T_+} - p|_{T_-}$ denote the jump of the piecewise polynomial $p \in RT_k(T)$ across an interior edge $E = \partial T_+ \cap \partial T_-$ shared by the two neighboring triangles T_+ and T_-. The Raviart–Thomas finite element space is defined as

$$RT_k(\mathcal{T}) := \{p \in H(\operatorname{div}, \Omega) \mid p|_T \in RT_k(T) \text{ for all } T \in \mathcal{T}\}$$
$$= \left\{p \in L^2(\Omega) \middle| \begin{array}{l} p|_T \in RT_k(\mathcal{T}) \text{ for all } T \in \mathcal{T}, \\ [p]_E \cdot \nu_E = 0 \text{ on } E \text{ for all } E \in \mathcal{E}(\Omega) \end{array}\right\}.$$

For piecewise constant $\varepsilon > 0$ on $\mathcal{T}$, the discrete formulation of (**D**$_\varepsilon$) reads as follows: Seek $(u_{\varepsilon h}, \sigma_{\varepsilon h}) \in \mathcal{P}_k(\mathcal{T}) \times RT_k(\mathcal{T})$ such that for all $(v_h, \tau_h) \in \mathcal{P}_k(\mathcal{T}) \times RT_k(\mathcal{T})$ it holds that

(**D**$_{\varepsilon h}$)
$$(\tau_h, D\Phi_\varepsilon^*(\sigma_{\varepsilon h}))_{L^2(\Omega)} + (u_{\varepsilon h}, \operatorname{div}\tau_h)_{L^2(\Omega)} = 0,$$
$$(v_h, \operatorname{div}\sigma_{\varepsilon h})_{L^2(\Omega)} + (f, v_h)_{L^2(\Omega)} = 0.$$

4. Existence of exact and discrete solutions. For the discrete form of the original primal problem (**P**) in section 3.1, the discrete primal stress

$$\sigma_h^P := \mathrm{D}\Phi_0\left(\nabla u_h^P\right) \in \mathcal{P}_0\left(\mathcal{T}; \mathbb{R}^2\right)$$

is a piecewise constant solution and existence of $u_h^P \in \mathcal{P}_1\left(\mathcal{T}\right) \cap V$ and the uniqueness of σ_h^P are clarified in [4]. In contrast to the continuous case, the primal and dual solutions of the discrete problem do not necessarily coincide and the first step is to prove existence of a discrete solution (u_h, σ_h) of the discrete form of the dual problem (**D**).

Let $f_h := \Pi_h f \in \mathcal{P}_k\left(\mathcal{T}\right) \subseteq L^2(\Omega)$ be the piecewise polynomial $L^2(\Omega)$ projection of f with respect to $\mathcal{T}$ of degree at most $k \geq 0$, and define

$$Q(f,\mathcal{T}) := \{\tau_h \in RT_k\left(\mathcal{T}\right) \mid f_h + \mathrm{div}\,\tau_h = 0 \text{ in } \Omega\},$$
$$Q(f) := \{\tau \in H(\mathrm{div}, \Omega) \mid f + \mathrm{div}\,\tau = 0\}.$$

Since $f \equiv 1 \equiv f_h$ in the optimal design problem (1.1), it holds that $Q(1, \mathcal{T}) = RT_k\left(\mathcal{T}\right) \cap Q(1)$.

Furthermore, let $\chi_{Q(f,\mathcal{T})}$ denote the indicator function (cf. [15]) of the convex subset $Q(f,\mathcal{T}) \subseteq RT_k\left(\mathcal{T}\right)$; i.e., for $\tau_h \in RT_k\left(\mathcal{T}\right)$,

$$\chi_{Q(f,\mathcal{T})}(\tau_h) := \begin{cases} 0 & \text{for } \tau_h \in Q(f,\mathcal{T}), \\ +\infty & \text{otherwise.} \end{cases}$$

THEOREM 4.1 (existence and uniqueness). *Let $\varepsilon \geq 0$ be piecewise constant with respect to $\mathcal{T}$. There exists a unique maximizer σ_ε of $E_\varepsilon^*(\tau) := -\int_\Omega \varphi_\varepsilon^*(|\tau|)\,\mathrm{dx}$, i.e.,*

$$E_\varepsilon^*(\tau) \leq E_\varepsilon^*(\sigma_\varepsilon) \quad \text{for all } \tau \in Q(f).$$

There exists a unique discrete maximizer σ_h of E_0^* in $Q(f,\mathcal{T})$, i.e.,

(4.1) $$E_0^*(\tau_h) \leq E_0^*(\sigma_h) \quad \text{for all } \tau_h \in Q(f,\mathcal{T}),$$

and for all $\varepsilon \geq 0$ there exists a unique maximizer $\sigma_{\varepsilon h}$ of E_ε^* in $Q(f,\mathcal{T})$, i.e.,

$$-E_\varepsilon^*(\sigma_{\varepsilon h}) \leq -E_\varepsilon^*(\tau_h) + \chi_{Q(f,\mathcal{T})}(\tau_h) \quad \text{for all } \tau_h \in RT_k\left(\mathcal{T}\right).$$

Furthermore, for $\varepsilon \geq 0$ piecewise constant with respect to $\mathcal{T}$ there exists some $u_{\varepsilon h}$ such that $(u_{\varepsilon h}, \sigma_{\varepsilon h})$ solves $(\mathbf{D}_{\varepsilon h})$. The Lagrange multiplier $u_{\varepsilon h}$ is unique for $\varepsilon > 0$.

Proof. The divergence operator $\mathrm{div} : H(\mathrm{div}, \Omega) \to L^2(\Omega)$ is linear and bounded. Hence, $Q(f)$ is a closed affine subspace. Since Φ_ε^* is a strongly convex function of quadratic growth on $H(\mathrm{div}, T)$ for all $T \in \mathcal{T}$, $-E_\varepsilon^*$ is strongly convex via

$$E_\varepsilon^*(\tau) = -\sum_{T \in \mathcal{T}} \int_T \Phi_\varepsilon^*(\tau)\,\mathrm{dx}$$

in $H(\mathrm{div}, \Omega)$ and there exists a unique maximizer σ_ε of E_ε^* in $Q(f)$. Furthermore, the intersection $Q(f,\mathcal{T}) := RT_k\left(\mathcal{T}\right) \cap Q(f)$ is a closed affine and finite-dimensional subspace and therefore convex and there exists a unique minimizer σ_h of $-E_0^*$ in $Q(f,\mathcal{T})$.

Similar arguments prove that $\sigma_{\varepsilon h}$ minimizes $-E_\varepsilon^*$ in $Q(f, \mathcal{T})$. Hence, [15, Theorem 2.32] verifies that

$$0 \in \partial(-E_\varepsilon^*(\sigma_{\varepsilon h})) + \partial \chi_{Q(f,\mathcal{T})}(\sigma_{\varepsilon h}).$$

This proves the existence and uniqueness of a discrete maximizer of E_ε^* for all $\varepsilon \geq 0$. Furthermore, there exists some $\xi_h \in \partial(-E_\varepsilon^*(\sigma_{\varepsilon h}))$ with $-\xi_h \in \partial \chi_{Q(f,\mathcal{T})}(\sigma_{\varepsilon h})$. The latter reads as

$$(-\xi_h, \tau - \sigma_{\varepsilon h})_{L^2(\Omega)} \leq 0 \quad \text{for all } \tau \in Q(f, \mathcal{T}).$$

Since $2\sigma_{\varepsilon h} - \tau \in Q(f, \mathcal{T})$ for all $\tau \in Q(f, \mathcal{T})$, the reverse inequality

$$(-\xi_h, \sigma_{\varepsilon h} - \tau)_{L^2(\Omega)} \leq 0$$

holds as well. Thus,

$$\xi_h \perp_{L^2(\Omega)} Q(0, \mathcal{T}), \quad \text{i.e.,} \quad Q(0, \mathcal{T}) \subseteq \ker \xi_h.$$

It is well known that the bilinear form $b : RT_k(\mathcal{T}) \times \mathcal{P}_k(\mathcal{T}) \to \mathbb{R}$ given by

$$b(q, v) := \int_\Omega v \operatorname{div} q \, \mathrm{d}x \quad \text{for all } q \in RT_k(\mathcal{T}), \, v \in \mathcal{P}_k(\mathcal{T})$$

fulfills the inf-sup condition. Therefore the operator B and its dual B^*,

$$B : Q(0, \mathcal{T})^\perp \to \mathcal{P}_k(\mathcal{T})^*, \qquad\qquad q \mapsto b(q, \cdot);$$
$$B^* : \mathcal{P}_k(\mathcal{T}) \to \left(Q(0, \mathcal{T})^\perp\right)^*, \qquad\qquad v_h \mapsto b(\cdot, v_h)|_{Q(0,\mathcal{T})^\perp},$$

with $Q(0, \mathcal{T})^\perp \equiv RT_k(\mathcal{T}) / Q(0, \mathcal{T})$, are isomorphisms [1]. For any $\xi_h \in Q(0, \mathcal{T})^\perp$ there exists a unique Riesz representation $u_{\varepsilon h} \in \mathcal{P}_0(\mathcal{T})$ with

$$(\xi_h, \tau_h)_{L^2(\Omega)} = B^*(u_{\varepsilon h})(\tau_h) \quad \text{for all } \tau_h \in Q(f, \mathcal{T})^\perp.$$

This implies that $(\sigma_{\varepsilon h}, u_{\varepsilon h})$ solves the problem $(\mathbf{D}_{\varepsilon h})$. While ξ_h and thus $u_{\varepsilon h}$ are unique for $\varepsilon > 0$; ξ_h and thus u_h may be nonunique for $\varepsilon = 0$. $\quad\square$

5. Error analysis. This section is devoted to the error analysis of $(\mathbf{D}_{\varepsilon h})$ by means of the lowest-order Raviart–Thomas finite element space $RT_k(\mathcal{T})$ for $k = 0$.

5.1. A priori regularization error analysis.
THEOREM 5.1. *For $\varepsilon > 0$ piecewise constant with respect to $\mathcal{T}$ and for $C_{reg} := \sqrt{C_\mu/(4\mu_2)}$ and $C_\mu > 0$ from Lemma 2.1, it holds that*

$$\|\sigma - \sigma_\varepsilon\|_{L^2(\Omega)} \leq C_{reg} \left\|\sqrt{\varepsilon}\sigma_\varepsilon\right\|_{L^2(\Omega)}$$
$$\leq C_{reg} \left\|\sqrt{\varepsilon}\sigma\right\|_{L^2(\Omega)} + C_{reg} \left\|\sqrt{\varepsilon}(\sigma - \sigma_\varepsilon)\right\|_{L^2(\Omega)}.$$

For sufficiently small maximal $\varepsilon_\infty = \|\varepsilon\|_\infty > 0$, it holds that

$$\|\sigma - \sigma_\varepsilon\|_{L^2(\Omega)} \leq \mathcal{O}(1) \left\|\sqrt{\varepsilon}\sigma\right\|_{L^2(\Omega)}.$$

Proof. Subsection 2.3(iv) ensures strong convexity of $\mathrm{D}\Phi^*_\varepsilon$ on all $T \in \mathcal{T}$, which implies strong convexity on Ω, i.e.,

$$2\mu_2 \left\|\sigma - \sigma_\varepsilon\right\|^2_{L^2(\Omega)} \le (\mathrm{D}\Phi^*_\varepsilon(\sigma_\varepsilon), \sigma - \sigma_\varepsilon)_{L^2(\Omega)} + \int_\Omega (\Phi^*_\varepsilon(\sigma) - \Phi^*_\varepsilon(\sigma_\varepsilon))\,\mathrm{dx},$$

$$2\mu_2 \left\|\sigma - \sigma_\varepsilon\right\|^2_{L^2(\Omega)} \le - (\partial\Phi^*_0(\sigma), \sigma - \sigma_\varepsilon)_{L^2(\Omega)} + \int_\Omega (\Phi^*_0(\sigma_\varepsilon) - \Phi^*_0(\sigma))\,\mathrm{dx}.$$

Hence, the preceding inequalities hold for all elements of the sets $\mathrm{D}\Phi^*_\varepsilon(\sigma_\varepsilon)$, $\partial\Phi^*_0(\sigma)$ such as $\nabla u_\varepsilon = \mathrm{D}\Phi^*_\varepsilon(\sigma_\varepsilon)$ and $\nabla u \in \partial\Phi^*_0(\sigma)$. An integration by parts shows that $(\nabla u, \sigma - \sigma_\varepsilon)_{L^2(\Omega)} = (\nabla u_\varepsilon, \sigma - \sigma_\varepsilon)_{L^2(\Omega)} = 0$. This implies that

$$4\mu_2 \left\|\sigma - \sigma_\varepsilon\right\|^2_{L^2(\Omega)} \le \int_\Omega (\Phi^*_\varepsilon(\sigma) - \Phi^*_0(\sigma) + \Phi^*_0(\sigma_\varepsilon) - \Phi^*_\varepsilon(\sigma_\varepsilon))\,\mathrm{dx}$$

$$\le \int_\Omega (\Phi^*_0(\sigma_\varepsilon) - \Phi^*_\varepsilon(\sigma_\varepsilon))\,\mathrm{dx}.$$

Recall that the Yosida regularization $\varphi^*_\varepsilon(t)$ of $\varphi^*_0(t)$ from Lemma 2.1 with $C_\mu > 0$ allows for the upper bounds

$$0 \le \varphi_0(t)^* - \varphi^*_\varepsilon(t) \le C_\mu \varepsilon t^2 \quad \text{for all } t \ge 0, \text{ with } C_\mu > 0,$$

$$0 \le \int_\Omega (\Phi^*_0(\tau) - \Phi^*_\varepsilon(\tau))\,\mathrm{dx} \le C_\mu \left\|\sqrt{\varepsilon}\tau\right\|^2_{L^2(\Omega)} \quad \text{for all } \tau \in L^2(\Omega; \mathbb{R}^2).$$

Therefore,

$$2\mu_2^{1/2} \left\|\sigma - \sigma_\varepsilon\right\|_{L^2(\Omega)} \le C_\mu^{1/2} \left\|\sqrt{\varepsilon}\sigma_\varepsilon\right\|_{L^2(\Omega)}$$

$$\le C_\mu^{1/2} \left\|\sqrt{\varepsilon}\sigma\right\|_{L^2(\Omega)} + C_\mu^{1/2} \left\|\sqrt{\varepsilon}(\sigma - \sigma_\varepsilon)\right\|_{L^2(\Omega)}.$$

Thus, for sufficiently small ε_∞, it holds that

$$\left\|\sigma - \sigma_\varepsilon\right\|_{L^2(\Omega)} \le \frac{1}{2\mu_2^{1/2}C_\mu^{-1/2} - \varepsilon_\infty^{1/2}} \left\|\sqrt{\varepsilon}\sigma\right\|_{L^2(\Omega)}. \qquad \square$$

5.2. A priori error analysis of spatial discretization. Let Ω_h denote the subset of all x in Ω where either $|\sigma_h(x)| \le t_1\mu_2 \le |\sigma(x)|$ or $|\sigma(x)| \le t_1\mu_2 \le |\sigma_h(x)|$:

$$\Omega_h := \{x \in \Omega \mid \min\{|\sigma(x)|, |\sigma_h(x)|\} \le t_1\mu_2 \le \max\{|\sigma(x)|, |\sigma_h(x)|\}\}.$$

Similarly, $\Omega_{\varepsilon h}$ denotes the subset of Ω of microstructure region for the regularized dual energy density function, i.e.,

$$\Omega_{\varepsilon h} := \left\{x \in \Omega \left| \begin{array}{l} \exists t \in t_1\mu_2 + \varepsilon[t_1, t_2] \text{ such that} \\ \min\{|\sigma_\varepsilon(x)|, |\sigma_{\varepsilon h}(x)|\} \le t \le \max\{|\sigma_\varepsilon(x)|, |\sigma_{\varepsilon h}(x)|\} \end{array} \right. \right\}.$$

The subsequent a priori error estimate leads to an estimate

(5.1) $$\|\sigma_\varepsilon - \sigma_{\varepsilon h}\|_{L^2(\Omega)} \lesssim H^{1/2}$$

for the dual solution $\sigma_\varepsilon \in H^1(\Omega; \mathbb{R}^2)$ and maximal mesh size $H := \max_{T \in \mathcal{T}} h_T$, $h_T := |T|^{1/2}$. For sufficient conditions for the H^1-regularity of the exact dual solution σ see [6].

THEOREM 5.2. *Let $f \in L^2(\Omega)$ be piecewise constant with respect to $\mathcal{T}$, and let $\sigma_\varepsilon \in H^1(\Omega; \mathbb{R}^2)$ be the exact dual solution of $(\mathbf{D}_\varepsilon)$. Then, the discrete solution $\sigma_{\varepsilon h}$ of $(\mathbf{D}_{\varepsilon h})$ on $\mathcal{T}$ for $\varepsilon > 0$ satisfies*

$$\|\sigma_\varepsilon - \sigma_{\varepsilon h}\|_{L^2(\Omega)} \lesssim H + H^{1/2} |\Omega_{\varepsilon h}|^{1/2}.$$

Before the proof of Theorem 5.2 concludes this section, some remarks are in order.

The numerical investigations in [18] are motivated by the following question: Does microstructure arise in this example in the sense that $\{|\sigma| = t_1\mu_2\}$ has a positive area? This zone of nontrivial Young measure solutions has been observed in the numerical simulations [4, 18] even though its area is usually very small. If the numerical approximation of this area is accurate, then $|\Omega_{\varepsilon h}| > 0$ and one cannot expect a higher convergence rate than that given in (5.1). Our numerical experiments shall investigate this as well as the preasymptotic behavior for small $|\Omega_{\varepsilon h}| / |\Omega| \ll 1$.

Proof of Theorem 5.2. Let $\mathrm{I}_F : H^1(\Omega; \mathbb{R}^2) \mapsto RT_0(\mathcal{T})$ be Fortin's interpolation operator [2, section III.3.3] with respect to $\mathcal{T}$ and be defined by

$$\int_E (\sigma_\varepsilon - \mathrm{I}_F\,\sigma_\varepsilon) \cdot \nu_E\,\mathrm{ds} = 0 \quad \text{for all } E \in \mathcal{E}.$$

Furthermore, let $\Pi_h : L^2(\Omega) \to \mathcal{P}_0(\mathcal{T})$ denote the L^2 projection. Besides the commuting diagram property $\mathrm{div}\,\mathrm{I}_F\,\sigma_\varepsilon = \Pi_h\,\mathrm{div}\,\sigma_\varepsilon$, the following estimates [2, section III.3.3] or [1, section III.5] hold on $T \in \mathcal{T}$:

$$(5.2) \qquad \|\mathrm{I}_F\,\sigma_\varepsilon - \sigma_\varepsilon\|_{L^2(T)} \lesssim h_T\,|\sigma_\varepsilon|_{H^1(T)}.$$

The strong monotonicity of Φ_ε^* of subsection 2.3(iii) on each $T \in \mathcal{T}$ yields

$$(5.3) \qquad \mu_2\,\|\sigma_\varepsilon - \sigma_{\varepsilon h}\|_{L^2(\Omega))}^2 \leq (\mathrm{D}\Phi_\varepsilon^*\,(\sigma_\varepsilon) - \mathrm{D}\Phi_\varepsilon^*\,(\sigma_{\varepsilon h}), \sigma_\varepsilon - \sigma_{\varepsilon h})_{L^2(\Omega)}.$$

Since $\sigma_{\varepsilon h}$, $I_F\sigma_\varepsilon \in Q(f) = Q(f, \mathcal{T})$ and $\mathrm{D}\Phi_\varepsilon^*(\sigma_\varepsilon) = \nabla u_\varepsilon$, the L^2-orthogonalities $\mathrm{D}\Phi_\varepsilon^*(\sigma_\varepsilon) \perp_{L^2(\Omega)} I_F(\sigma_\varepsilon - \sigma_{\varepsilon h})$ and $u_{\varepsilon h} \perp_{L^2(\Omega)} \mathrm{div}(\sigma_{\varepsilon h} - I_F\sigma_\varepsilon)$ hold. Hence, (5.2)–(5.3) prove

$$\mu_2\,\|\sigma_\varepsilon - \sigma_{\varepsilon h}\|_{L^2(\Omega))}^2 \leq (\mathrm{D}\Phi_\varepsilon^*\,(\sigma_{\varepsilon h}), \mathrm{I}_F\,\sigma_\varepsilon - \sigma_\varepsilon)_{L^2(\Omega)} - (u_{\varepsilon h}, \mathrm{div}\,(\sigma_\varepsilon - \mathrm{I}_F\,\sigma_\varepsilon))_{L^2(\Omega)}.$$

Furthermore, since $\mathrm{div}(\mathrm{I}_F\,\sigma_\varepsilon - \sigma_\varepsilon) = f - f_h = 0$ for piecewise constant f and $0 = (u_{\varepsilon h}, \mathrm{div}(\sigma_\varepsilon - I_F\sigma_\varepsilon))_{L^2(\Omega)}$, the following estimate holds:

$$\mu_2\,\|\sigma_\varepsilon - \sigma_{\varepsilon h}\|_{L^2(\Omega))}^2 \leq (\mathrm{D}\Phi_\varepsilon^*\,(\sigma_{\varepsilon h}), \mathrm{I}_F\,\sigma_\varepsilon - \sigma_\varepsilon)_{L^2(\Omega)} + (u_h, \mathrm{div}\,(\mathrm{I}_F\,\sigma_\varepsilon - \sigma_\varepsilon))_{L^2(\Omega)}$$
$$= (\mathrm{D}\Phi_\varepsilon^*\,(\sigma_{\varepsilon h}) - \mathrm{D}\Phi_\varepsilon^*\,(\sigma_\varepsilon), \mathrm{I}_F\,\sigma_\varepsilon - \sigma_\varepsilon)_{L^2(\Omega)}.$$

Cauchy–Schwarz's inequality, subsection 2.3(vi), and the estimates of Fortin's interpolation with $C_{\mathrm{F}} > 0$ lead to

$$\mu_2\,\|\sigma_\varepsilon - \sigma_{\varepsilon h}\|_{L^2(\Omega)}^2 \leq \|\mathrm{D}\Phi_\varepsilon^*\,(\sigma_{\varepsilon h}) - \mathrm{D}\Phi_\varepsilon^*\,(\sigma_\varepsilon)\|_{L^2(\Omega)}\,\|\mathrm{I}_F\,\sigma_\varepsilon - \sigma_\varepsilon\|_{L^2(\Omega)}$$
$$\leq \left(\|\delta_\varepsilon\,(\sigma_\varepsilon, \sigma_{\varepsilon h})\|_{L^2(\Omega)} + 1/\mu_1\,\|\sigma_\varepsilon - \sigma_{\varepsilon h}\|_{L^2(\Omega)}\right) C_{\mathrm{F}} H\,|\sigma_\varepsilon|_{H^1(\Omega)}.$$

With $\Omega_{\varepsilon h}$ from the beginning of this subsection and subsection 2.3(vi) in the sense of

$$\|\delta_\varepsilon\,(\sigma_\varepsilon, \sigma_{\varepsilon h})\|_{L^2(\Omega)} \leq |\Omega_{\varepsilon h}|\,(t_2 - t_1) \lesssim 1,$$

one concludes that

$$\mu_2 \left\| \sigma_\varepsilon - \sigma_{\varepsilon h} \right\|_{L^2(\Omega)}^2 \leq H C_{\mathrm{F}} \left(t_2 - t_1 \right) \left| \Omega_{\varepsilon h} \right| \left| \sigma_\varepsilon \right|_{H^1(\Omega)}$$
$$+ H C_{\mathrm{F}} / \mu_1 \left\| \sigma_\varepsilon - \sigma_{\varepsilon h} \right\|_{L^2(\Omega)} \left| \sigma_\varepsilon \right|_{H^1(\Omega)}.$$

Young's inequality proves the assertion

$$\left\| \sigma_\varepsilon - \sigma_{\varepsilon h} \right\|_{L^2(\Omega)}^2 \lesssim H \left| \Omega_{\varepsilon h} \right| \left| \sigma_\varepsilon \right|_{H^1(\Omega)} + H^2 \left| \sigma_\varepsilon \right|_{H^1(\Omega)}^2 \lesssim H \left| \Omega_{\varepsilon h} \right| + H^2. \qquad \square$$

5.3. A posteriori error analysis.

THEOREM 5.3. *For the exact and discrete solutions $\sigma_\varepsilon \in H^1(\Omega; \mathbb{R}^2)$ and $\sigma_{\varepsilon h} \in RT_0(\mathcal{T})$ of $(\mathbf{D}_\varepsilon)$ and $(\mathbf{D}_{\varepsilon h})$, $\varepsilon > 0$ with piecewise constant right-hand side $f \in L^2(\Omega)$ with respect to $\mathcal{T}$, and for $C := C_C(1 + C_{reg}\sqrt{\varepsilon_\infty})$ and for positive constants C_{reg} of Theorem 5.1 and C_C of Clément's interpolation, it holds that*

$$\left\| \sigma - \sigma_{\varepsilon h} \right\|_{L^2(\Omega)}$$
(5.4)
$$\leq C_{reg} \left\| \sqrt{\varepsilon}\sigma_{\varepsilon h} \right\|_{L^2(\Omega)} + 1/\mu_2 \min_{v \in V} \left\| \mathrm{D}\Phi_\varepsilon^* \left(\left| \sigma_{\varepsilon h} \right| \right) - \nabla v \right\|_{L^2(\Omega)}$$

$$\leq C_{reg} \left\| \sqrt{\varepsilon}\sigma_{\varepsilon h} \right\|_{L^2(\Omega)} + C/\mu_2 \left(\sum_{E \in \mathcal{E}} \left\| h_E^{1/2} \left[\mathrm{D}\Phi_\varepsilon^* \left(\sigma_{\varepsilon h} \right) \right] \cdot \tau_E \right\|_{L^2(E)} \right.$$
(5.5)
$$+ \sum_{T \in \mathcal{T}} \left\| h_T \operatorname{curl} \mathrm{D}\Phi_\varepsilon^* \left(\sigma_{\varepsilon h} \right) \right\|_{L^2(T)} \right).$$

Proof. The triangle inequality and the estimates of Theorem 5.1 reveal that

$$\left\| \sigma - \sigma_{\varepsilon h} \right\|_{L^2(\Omega)} \leq \left\| \sigma - \sigma_\varepsilon \right\|_{L^2(\Omega)} + \left\| \sigma_\varepsilon - \sigma_{\varepsilon h} \right\|_{L^2(\Omega)}$$
$$\leq C_{reg} \left\| \sqrt{\varepsilon}\sigma_\varepsilon \right\|_{L^2(\Omega)} + \left\| \sigma_\varepsilon - \sigma_{\varepsilon h} \right\|_{L^2(\Omega)}$$
$$\leq C_{reg} \left\| \sqrt{\varepsilon}\sigma_{\varepsilon h} \right\|_{L^2(\Omega)} + \left\| \left(1 + C_{reg}\sqrt{\varepsilon} \right) \left(\sigma_\varepsilon - \sigma_{\varepsilon h} \right) \right\|_{L^2(\Omega)}.$$

Furthermore, the inequality of subsection 2.3(iii) leads for $\varepsilon > 0$ to

$$\mu_2 \left\| \sigma_\varepsilon - \sigma_{\varepsilon h} \right\|_{L^2(\Omega)}^2 \leq \left(\mathrm{D}\Phi_\varepsilon^* \left(\sigma_\varepsilon \right) - \mathrm{D}\Phi_\varepsilon^* \left(\sigma_{\varepsilon h} \right), \sigma_\varepsilon - \sigma_{\varepsilon h} \right)_{L^2(\Omega)}.$$

Since $\nabla u_\varepsilon = \mathrm{D}\Phi_\varepsilon^* \left(\sigma_\varepsilon \right)$, the right-hand side equals

$$\left(\nabla u_\varepsilon - \mathrm{D}\Phi_\varepsilon^* \left(\sigma_{\varepsilon h} \right), \sigma_\varepsilon - \sigma_{\varepsilon h} \right)_{L^2(\Omega)}.$$

An integration by parts with $u_\varepsilon \in V$ shows that this equals

$$\left(u_\varepsilon, \operatorname{div} \left(\sigma_{\varepsilon h} - \sigma_\varepsilon \right) \right)_{L^2(\Omega)} - \left(\mathrm{D}\Phi_\varepsilon^* \left(\sigma_{\varepsilon h} \right), \sigma_\varepsilon - \sigma_{\varepsilon h} \right)_{L^2(\Omega)}.$$

Since $\operatorname{div} \left(\sigma_\varepsilon - \sigma_{\varepsilon h} \right) = f - f_h \equiv 0$ for piecewise constant f, the first term vanishes. The same argument for any $v \in V$ results in

$$\mu_2 \left\| \sigma_\varepsilon - \sigma_{\varepsilon h} \right\|_{L^2(\Omega)}^2 \leq \left(\nabla v - \mathrm{D}\Phi_\varepsilon^* \left(\sigma_{\varepsilon h} \right), \sigma_\varepsilon - \sigma_{\varepsilon h} \right)_{L^2(\Omega)}$$
$$\leq \left\| \mathrm{D}\Phi_\varepsilon^* \left(\sigma_{\varepsilon h} \right) - \nabla v \right\|_{L^2(\Omega)} \left\| \sigma_\varepsilon - \sigma_{\varepsilon h} \right\|_{L^2(\Omega)}.$$

Hence,

$$\mu_2 \left\| \sigma_\varepsilon - \sigma_{\varepsilon h} \right\|_{L^2(\Omega)} \leq \min_{v \in V} \left\| \mathrm{D}\Phi_\varepsilon^* \left(\sigma_{\varepsilon h} \right) - \nabla v \right\|_{L^2(\Omega)}.$$

Define $\tilde{v} := \operatorname{argmin}_{v \in V} \left\| \mathrm{D}\Phi_\varepsilon^* \left(\sigma_{\varepsilon h} \right) - \nabla v \right\|_{L^2(\Omega)}$ so that $\tilde{v} \in V$ satisfies

(5.6) $$\left(\nabla \tilde{v}, \nabla w \right)_{L^2(\Omega)} = \left(\mathrm{D}\Phi_\varepsilon^* \left(\sigma_{\varepsilon h} \right), \nabla w \right)_{L^2(\Omega)} \quad \text{for all } w \in V.$$

The Helmholtz decomposition [12] of $\mathrm{D}\Phi_\varepsilon^* \left(\sigma_{\varepsilon h} \right)$ in $\alpha \in V$ and $\beta \in H^1(\Omega)/\mathbb{R}$ reads as

(5.7) $$\mathrm{D}\Phi_\varepsilon^* \left(\sigma_{\varepsilon h} \right) = \nabla \alpha + \operatorname{Curl} \beta$$

with an orthogonal split $\left(\nabla \alpha, \operatorname{Curl} \beta \right)_{L^2(\Omega)} = 0$. Hence,

$$\mu_2 \left\| \sigma_\varepsilon - \sigma_{\varepsilon h} \right\|_{L^2(\Omega)} \leq \left\| \mathrm{D}\Phi_\varepsilon^* \left(\sigma_{\varepsilon h} \right) - \nabla \tilde{v} \right\|_{L^2(\Omega)} = \left\| \operatorname{Curl} \beta \right\|_{L^2(\Omega)}.$$

For $z \in \mathcal{N}$ define $\omega_z := \{ T \in \mathcal{T} \mid z \in T \}$ as the patch to the node z. Define the nodal function $\phi_z \in \mathcal{S}_1 \left(\mathcal{T} \right)$ by $\phi_z(z) := 1$ for $z \in \mathcal{N}$ and $\phi_z(y) = 0$ for $y \in \mathcal{N} \setminus \{z\}$.

Let $J : H^1(\Omega) \to \mathcal{S}_1 \left(\mathcal{T} \right)$ be the Clément-interpolation operator and $J\beta$ be the interpolator of β given by [2]

$$J \left(\beta \right) := \sum_{z \in \mathcal{N}} \beta_z \phi_z \text{ with } \beta_z := \begin{cases} \left| \omega_z \right|^{-1} \int_{\omega_z} \beta \, \mathrm{d}x & \text{for all } z \in \mathcal{N} \setminus \partial\Omega, \\ 0 & \text{for all } z \in \mathcal{N} \cap \partial\Omega. \end{cases}$$

Thus, $\operatorname{Curl} J\beta \in \mathcal{P}_0 \left(\mathcal{T} \right) \cap H \left(\operatorname{div}, \Omega \right) \subset RT_0 \left(\mathcal{T} \right)$ and for $\beta \in H^1(\Omega)$ the following estimates hold [10]:

$$\left\| \nabla J \left(\beta \right) \right\|_{L^2(\Omega)} + \left\| h_{\mathcal{T}}^{-1} \left(\beta - J \left(\beta \right) \right) \right\|_{L^2(\Omega)} + \left\| h_{\mathcal{E}}^{-1/2} \left(\beta - J \left(\beta \right) \right) \right\|_{L^2(\cup \mathcal{E})} \lesssim \left\| \nabla \beta \right\|_{L^2(\Omega)}.$$

Let $[J\beta] \cdot \nu$ denote the jump of $J\beta$ in the normal direction across (and $[J\beta] \cdot \tau$ in the tangential direction along) the edges in $\mathcal{E}$. Hence, $\left| [\operatorname{Curl} J\beta] \cdot \nu \right|_{\mathcal{E}} = \left| [J\beta] \cdot \tau \right|_{\mathcal{E}} = 0$.

Since $\operatorname{Curl} J\beta \perp \nabla H_0^1 \left(\Omega \right)$ and $\left(\mathrm{D}\Phi_\varepsilon^* \left(\sigma_{\varepsilon h} \right), q_h \right) = \left(-u_{\varepsilon h}, \operatorname{div} q_h \right)$ hold for all $q_h \in RT_0 \left(\mathcal{T} \right)$, the orthogonal split $\operatorname{Curl} \beta \perp \operatorname{Curl} J\beta$ is verified:

$$\left(\operatorname{Curl} \beta, \operatorname{Curl} J\beta \right)_{L^2(\Omega)} = \left(\mathrm{D}\Phi_\varepsilon^* \left(\sigma_{\varepsilon h} \right) - \nabla \alpha, \operatorname{Curl} J\beta \right)_{L^2(\Omega)}$$
$$= - \left(u_{\varepsilon h}, \operatorname{div} \operatorname{Curl} J\beta \right)_{L^2(\Omega)} = 0.$$

Let $C_{\mathrm{C}} > 0$ be a constant from Clément's interpolation error estimates. The orthog-

onality $\operatorname{Curl}\beta \perp \operatorname{Curl}J\beta$ yields

$$
\begin{aligned}
\|\operatorname{Curl}\beta\|_{L^2(\Omega)}^2 &= (\mathrm{D}\Phi_\varepsilon^*(\sigma_{\varepsilon h}) - \nabla\alpha, \operatorname{Curl}(\beta - J\beta))_{L^2(\Omega)} \\
&= \sum_{T\in\mathcal{T}} \Big(-\left(\operatorname{curl}\mathrm{D}\Phi_\varepsilon^*(\sigma_{\varepsilon h}), \beta - J\beta\right)_{L^2(T)} \\
&\qquad\qquad + \left(\mathrm{D}\Phi_\varepsilon^*(\sigma_{\varepsilon h})\cdot\tau, \beta - J\beta\right)_{L^2(\partial T)} \Big) \\
&\leq \sum_{T\in\mathcal{T}} \|h_T\operatorname{curl}\mathrm{D}\Phi_\varepsilon^*(\sigma_{\varepsilon h})\|_{L^2(T)} \left\|h_T^{-1}(\beta - J\beta)\right\|_{L^2(T)} \\
&\qquad + \sum_{E\in\mathcal{E}} \left\|h_E^{1/2}[\mathrm{D}\Phi_\varepsilon^*(\sigma_{\varepsilon h})]\cdot\tau_E\right\|_{L^2(E)} \left\|h_E^{-1/2}(\beta - J\beta)\right\|_{L^2(E)} \\
&\leq C_{\mathrm{C}} \left(\sum_{T\in\mathcal{T}} \|h_T\operatorname{curl}\mathrm{D}\Phi_\varepsilon^*(\sigma_{\varepsilon h})\|_{L^2(T)}^2 \right. \\
&\qquad\qquad \left. + \sum_{E\in\mathcal{E}} \left\|h_E^{1/2}[\mathrm{D}\Phi_\varepsilon^*(\sigma_{\varepsilon h})]\cdot\tau_E\right\|_{L^2(E)}^2 \right)^{1/2} \|\nabla\beta\|_{L^2(\Omega)}.
\end{aligned}
$$

Finally, $\|\nabla\beta\|_{L^2(\Omega)} = \|\operatorname{Curl}\beta\|_{L^2(\Omega)}$ shows the assertion. ☐

Remark 5.4. Given the definition of φ_0^* from the variational formulation of the optimal design example in section 2.1 and its regularization φ_ε^*, one observes that $\mathrm{D}\Phi_\varepsilon^*(\sigma_{\varepsilon h})$ is a Raviart–Thomas element shape function in the interior of each material Ω_1 and Ω_2, where $\operatorname{curl}\mathrm{D}\Phi_\varepsilon^*(\sigma_{\varepsilon h}) = 0$.

Hence, the elements T in a neighborhood of the contact zone of the two materials exclusively contribute to $\sum_{T\in\mathcal{T}} \|h_T\operatorname{curl}\mathrm{D}\Phi_\varepsilon^*(\sigma_{\varepsilon h})\|_{L^2(T)}^2$ and the jump term in (5.5) may dominate the error estimator.

Remark 5.5. The right-hand side in (5.4)–(5.5) is expected to be sharp in the sense that the arguments are known to lead to efficient error control in many applications of MFEMs. Standard techniques for an efficiency proof, however, encounter the nonsmoothness of $\mathrm{D}\Phi_\varepsilon^*$ as $\varepsilon \searrow 0$.

6. Numerical experiments. This section is devoted to numerical experiments for the degenerate variational problem in its dual discrete mixed formulation $(\mathbf{D}_{\varepsilon h})$ based on the Raviart–Thomas FEM in comparison to the discrete solutions of $(\mathbf{P})$ in [4] with the P_1-FEM on the domains of Figure 6.1: the square, the L-shaped domain, and the octagon. In all of these examples the loads and the boundary conditions are given by $f \equiv 1$ and $u_D \equiv 0$. The material distribution is set to $\xi = 0.5$; thus both materials fill half of the domain, with the material parameters $\mu_1 = 1 < \mu_2 = 2$.

6.1. Preliminary remarks. In the variational formulation of the primal problem the Lagrange multiplier for the material distribution is λ; cf. [4] for a motivation and the computation of the optimal values shown in Figure 6.1.

However, an approximation of the exact primal and conjugated energy seems very discerning. The arduousness lies in the fact that extrapolation is significant only on uniform meshes, while for uniformly refined meshes the contact zone of both materials in the cross section is not adequately resolved. Thus, only a low number of digits appears trustworthy. This leads to objectionable effects in the convergence graphs of the approximation of the energy error. The extrapolation of sequences of
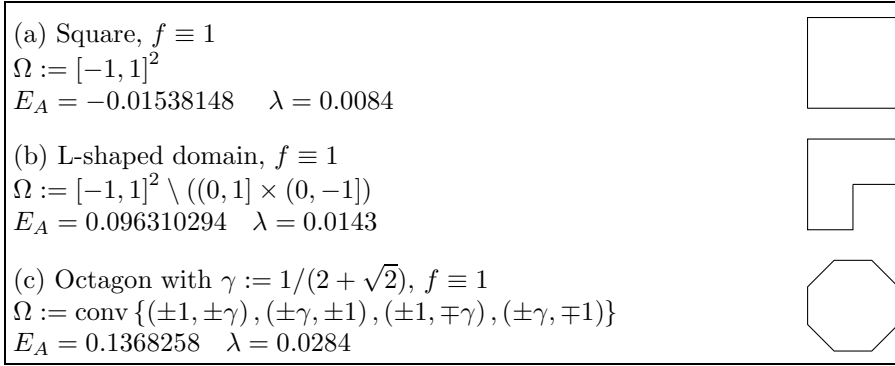
(a) Square, $f \equiv 1$
$\Omega := [-1, 1]^2$
$E_A = -0.01538148 \quad \lambda = 0.0084$

(b) L-shaped domain, $f \equiv 1$
$\Omega := [-1, 1]^2 \setminus ((0, 1] \times (0, -1])$
$E_A = 0.096310294 \quad \lambda = 0.0143$

(c) Octagon with $\gamma := 1/(2 + \sqrt{2})$, $f \equiv 1$
$\Omega := \mathrm{conv} \{(\pm 1, \pm \gamma), (\pm \gamma, \pm 1), (\pm 1, \mp \gamma), (\pm \gamma, \mp 1)\}$
$E_A = 0.1368258 \quad \lambda = 0.0284$

FIG. 6.1. *Domains of the four numerical benchmarks, their extrapolated energies E_A (rounded off), and their optimal λ.*

the dual energy

$$E_\varepsilon^* := \int_\Omega \varphi_\varepsilon^* (|\sigma_h|)\, \mathrm{dx} \quad \text{for } \varepsilon \geq 0$$

on uniform meshes based on the dual mixed formulation $(\mathbf{D}_{\varepsilon h})$ appears unreliable. The listed extrapolated energies E_A have been calculated by some Aitken extrapolation algorithm on uniform refined meshes, generated by the $\mathcal{S}_1$ conforming FEM based on the discrete form of the primal problem $(\mathbf{P})$ as in [4].

The analysis of section 5 motivates the following two estimators η_H and η_R for $\varepsilon > 0$:

(6.1)
$$\eta_H^2 := \min_{v \in \mathcal{S}_{1,0}(\mathcal{T})} \|\mathrm{D}\Phi_\varepsilon^*(\sigma_{\varepsilon h}) - \nabla v\|_{L^2(\mathcal{T})}^2 ,$$

$$\eta_\mathcal{E}^2 := \sum_{E \in \mathcal{E}} \left\| h_E^{1/2} \left[\mathrm{D}\Phi_\varepsilon^*(\sigma_{\varepsilon h})\right] \cdot \tau_E \right\|_{L^2(E)}^2 ,$$

(6.2)
$$\eta_R^2 := \eta_\mathcal{E}^2 + \sum_{T \in \mathcal{T}} \|h_T \operatorname{curl} \mathrm{D}\Phi_\varepsilon^*(\sigma_{\varepsilon h})\|_{L^2(T)}^2 .$$

Since the exact solution is not available, the convergence behavior of the estimators (6.1) and (6.2) is compared for adaptive and uniform mesh refinement.

The following algorithm solves $(\mathbf{D}_{\varepsilon h})$ and decreases ε locally for an accurate computation.

ALGORITHM 6.1. *Input: shape regular triangulation $\mathcal{T}_0$, initial value $(u_{\varepsilon 0}, \sigma_{\varepsilon 0})$, regularization parameters α and β, tolerance $0 < \mathrm{Tol}$. Set $\eta_0 := \infty$, $\ell := 1$.*
WHILE $\eta_{\ell-1} \geq \mathrm{Tol}$ **DO** (i)–(v):
  (i) *Create new triangulation $\mathcal{T}_\ell$ corresponding to the estimated error η_ℓ.*
  (ii) *Prolongate $(u_{\varepsilon \ell-1}, \sigma_{\varepsilon \ell-1})$ to $\mathcal{T}_\ell$ to get an initial value $(u_{\varepsilon \ell}^0, \sigma_{\varepsilon \ell}^0)$.*
  (iii) *Update regularization parameter $\varepsilon_{|_T} = \alpha h_T^\beta$, $T \in \mathcal{T}_\ell$.*
  (iv) *Compute solution $(u_{\varepsilon \ell}, \sigma_{\varepsilon \ell})$ of $(\mathbf{D}_{\varepsilon h})$ with the Gauss–Newton method provided in $\mathtt{fsolve}$ of MATLAB and initial value $(u_{\varepsilon \ell}^0, \sigma_{\varepsilon \ell}^0)$.*
  (v) *Calculate estimated error η_ℓ of the solution $\sigma_{\varepsilon \ell}$, and set $\ell = \ell + 1$.*
Output: Approximation of the solution of $(\mathbf{D}_{\varepsilon h})$.

Remark 6.2. The estimates $\|\sigma - \sigma_\varepsilon\|_{L^2(\Omega)} \lesssim \|\sqrt{\varepsilon}\sigma_\varepsilon\|_{L^2(\Omega)}$ and $\|\sigma_\varepsilon - \sigma_{\varepsilon h}\|_{L^2(\Omega)} \lesssim$ $H^{1/2}$ from Theorems 5.1 and 5.2 suggest $\varepsilon = \mathcal{O}(h)$. To find appropriate values of α
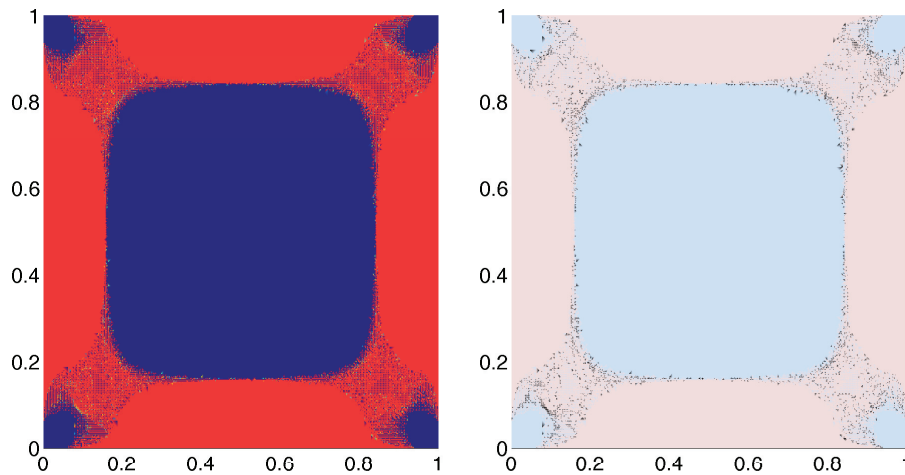
FIG. 6.2. *Left: Volume fraction for the two materials (blue and red) for adaptive refinement for the square generated by Algorithm 6.1 and η_R. Right: The region of microstructure as the approximated mixed zone where both materials are present (black).*

and β in the ansatz $\varepsilon|_T := \alpha h_T^\beta$, Algorithm 6.1 has run for various choices of α and β on the test setting on the unit square Ω with the exact solution

(6.3) $$\tilde{u}(x, y) := x\,y\,(1 - x)\,(1 - y).$$

The error estimators η_H and η_R, the exact stress errors $\|\sigma - \sigma_{\varepsilon h}\|_{L^2(\Omega)}$, and the square root of the energy error $\delta_\ell := |E(\sigma_{\varepsilon h}) - E_A|$ have been evaluated for various parameters and have led to the conjecture that $\alpha = \beta = 1$ is a proper choice for the regularization parameter $\varepsilon = h_T$ in Algorithm 6.1.

6.2. Optimal design on different domains. To analyze the quality of results produced by Algorithm 6.1, it is applied to the examples introduced in Figure 6.1. For each domain, the exact energy is approximated by an Aitken extrapolation of the discrete energy; this extrapolated energy E_A is given in Figure 6.1.

For each domain, the subsequent figures show the approximated optimal volume fraction

$$\begin{cases} 0 & \text{for } 0 \le |\nabla u_{\varepsilon h}| \le t_1, \\ (|\nabla u_{\varepsilon h}| - t_1)/(t_2 - t_1) & \text{for } t_1 \le |\nabla u_{\varepsilon h}| \le t_2, \\ 1 & \text{for } t_2 \le |\nabla u_{\varepsilon h}| \end{cases}$$

of each material indicated by regions colored red and blue on the left-hand side and the region of microstructure where both materials are present in black on the right-hand side. The estimated errors η_H, η_R and square root of the energy error for sequences of uniform and adaptively generated triangulations are plotted depending on the number of degrees of freedom (ndof). Furthermore a subsequence of the η_H-adaptively generated grids is shown. For the square domain those results are presented in Figures 6.2–6.4, for the L-shaped domain in Figures 6.5–6.8, for the octagon domain in Figures 6.9–6.12, and for all benchmark domains in Figures 6.13–6.14.
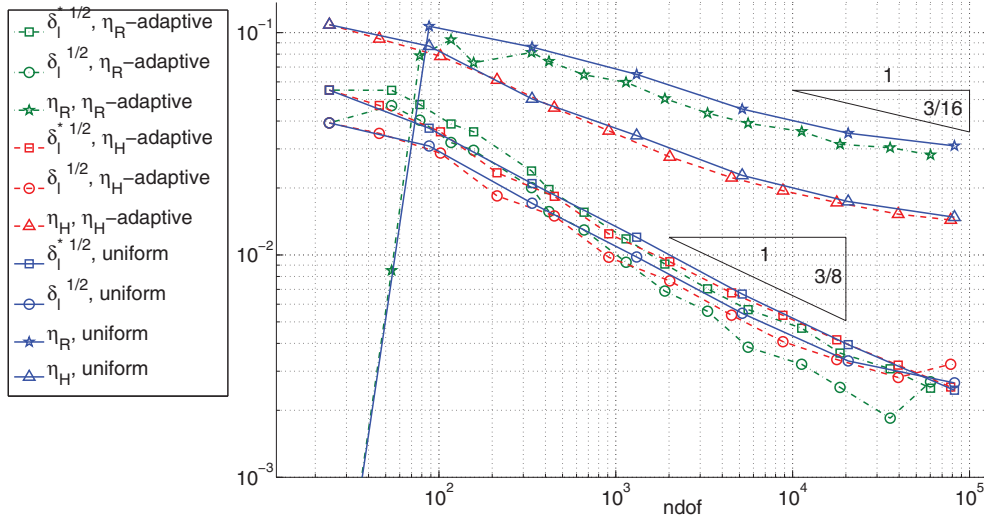
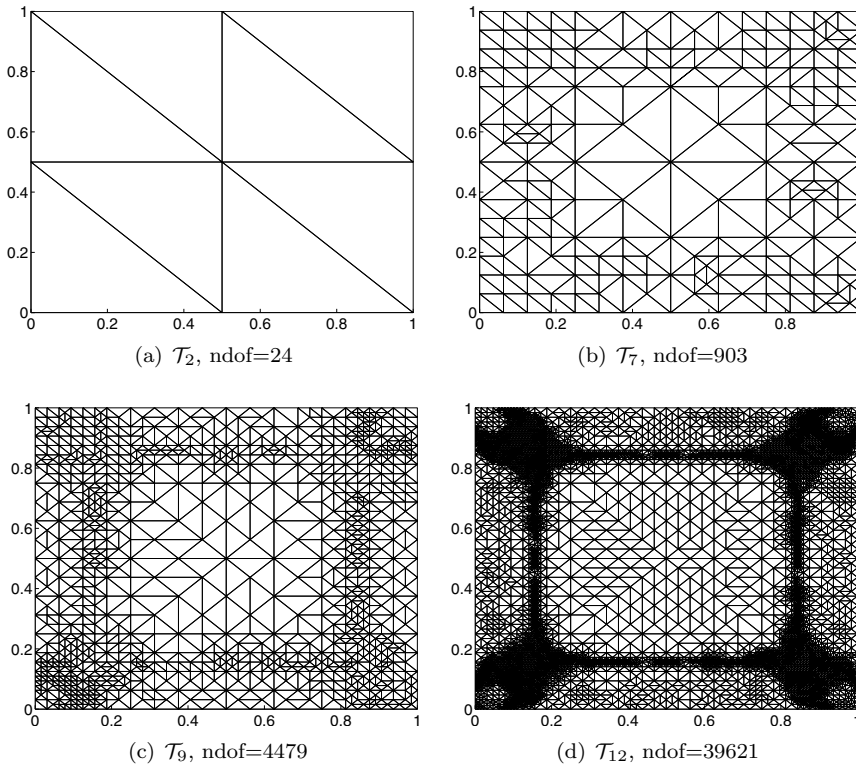FIG. 6.3. *Convergence history; error estimators and extrapolated energy error for the square.*

(a) $\mathcal{T}_2$, ndof=24

(b) $\mathcal{T}_7$, ndof=903

(c) $\mathcal{T}_9$, ndof=4479

(d) $\mathcal{T}_{12}$, ndof=39621

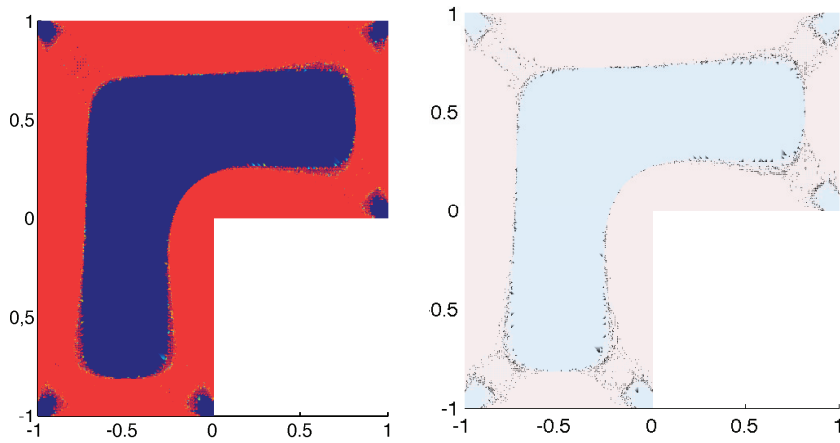FIG. 6.4. *Sequence of meshes generated by Algorithm* 6.1 *and* η_H *for the square.*

FIG. 6.5. *Volume fraction for uniform refinement for the L-shaped domain generated by Algorithm* 6.1 *and* η_R *(left) and its microstructure (right).*
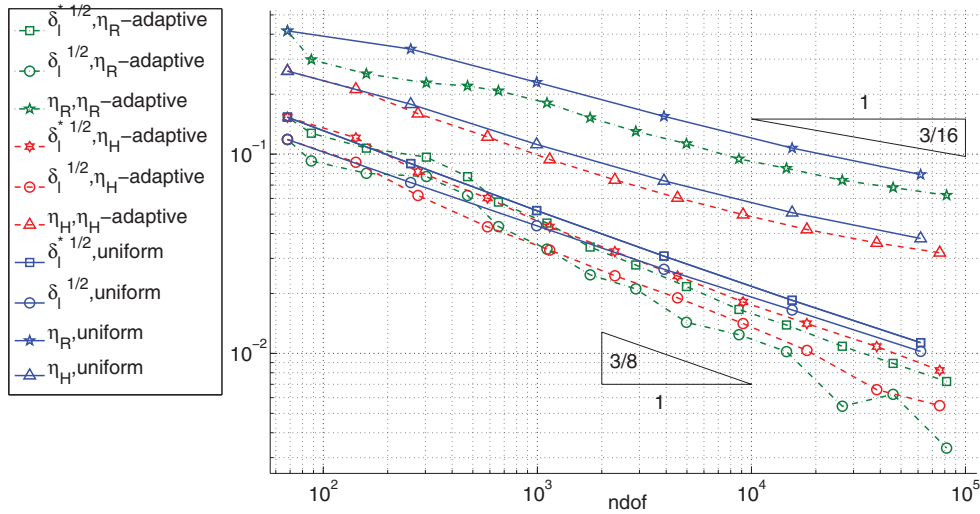

FIG. 6.6. *Convergence history; error estimators and extrapolated energy error for the L-shaped domain.*
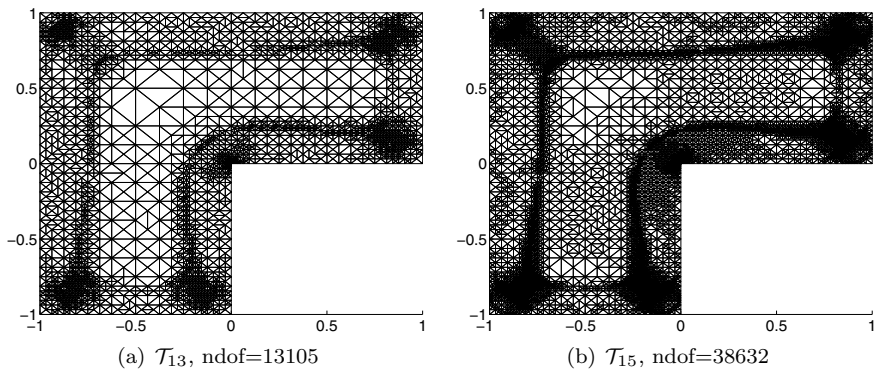
(a) $\mathcal{T}_{13}$, ndof=13105   (b) $\mathcal{T}_{15}$, ndof=38632

FIG. 6.7. *Subsequence of meshes of the L-shaped domain generated by Algorithm* 6.1 *and* η_R.

(a) $\mathcal{T}_{10}$, ndof=18142

(b) $\mathcal{T}_{12}$, ndof=77543
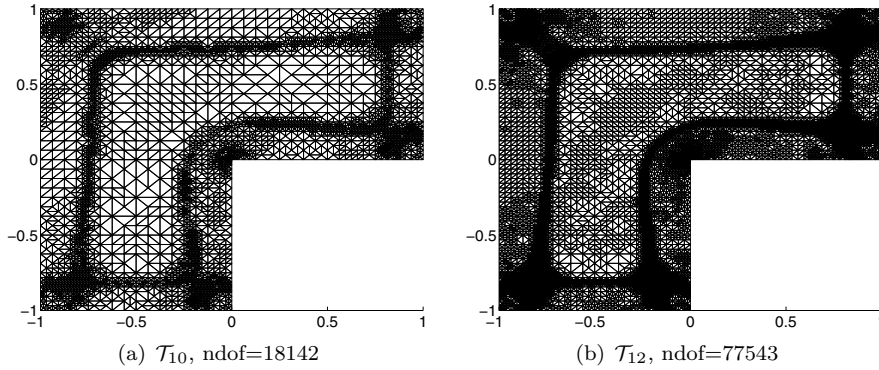
Fig. 6.8. *Subsequence of meshes of the L-shaped domain generated by Algorithm* 6.1 *and* η_H.
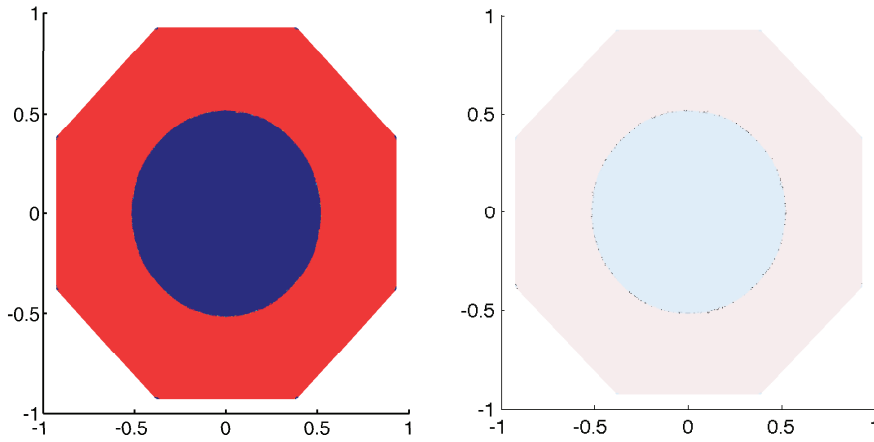
Fig. 6.9. *Volume fraction for uniform refinement for the octagon generated by Algorithm* 6.1 *and* η_R.
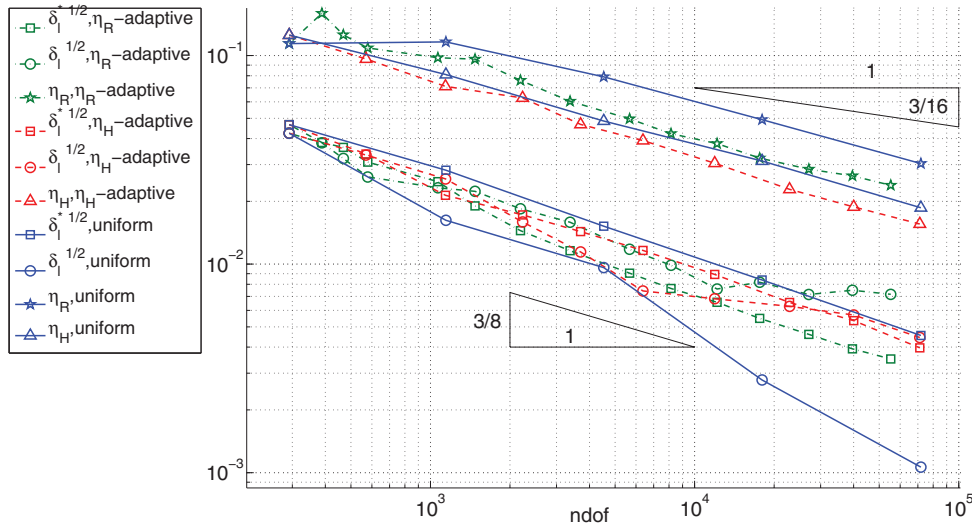

Fig. 6.10. *Convergence history; error estimators and extrapolated energy error for the octagon.*
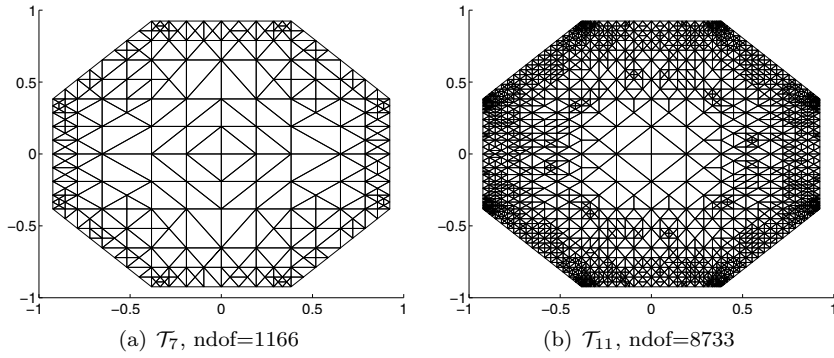
(a) $\mathcal{T}_7$, ndof=1166   (b) $\mathcal{T}_{11}$, ndof=8733

Fig. 6.11. *Subsequence of meshes generated by Algorithm* 6.1 *and* η_R *for the octagon.*

(a) $\mathcal{T}_7$, ndof=7352   (b) $\mathcal{T}_9$, ndof=26214
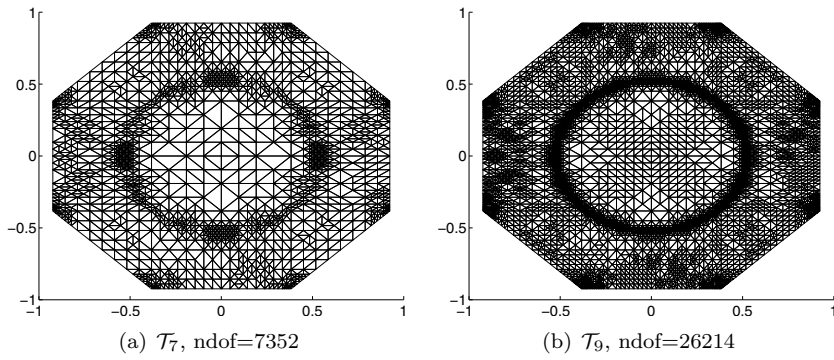
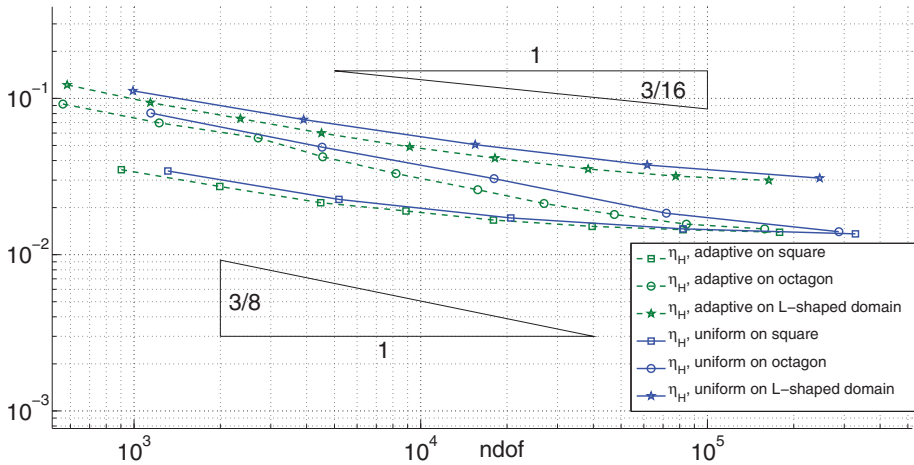Fig. 6.12. *Subsequence of meshes generated by Algorithm* 6.1 *and* η_H *for the octagon.*

Fig. 6.13. *Convergence history of* η_H *for adaptive and uniform refinement on all benchmark domains.*
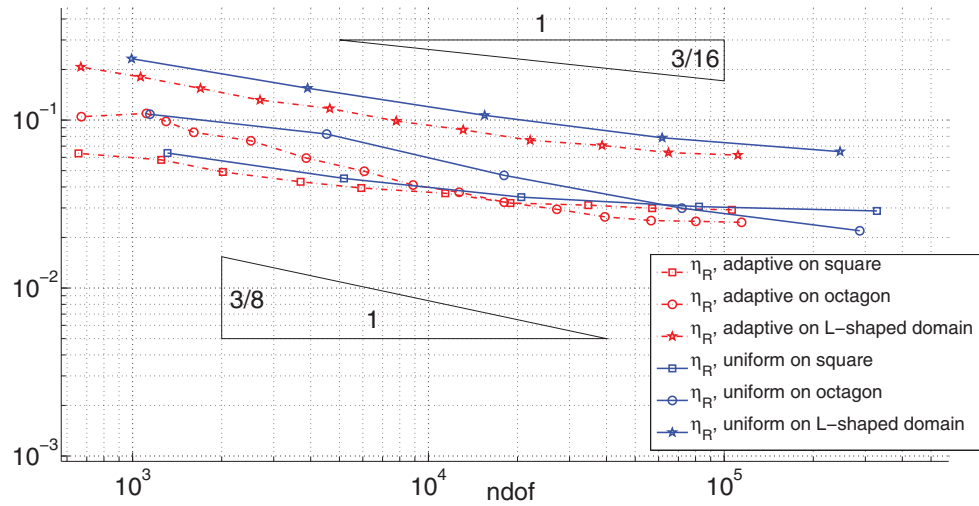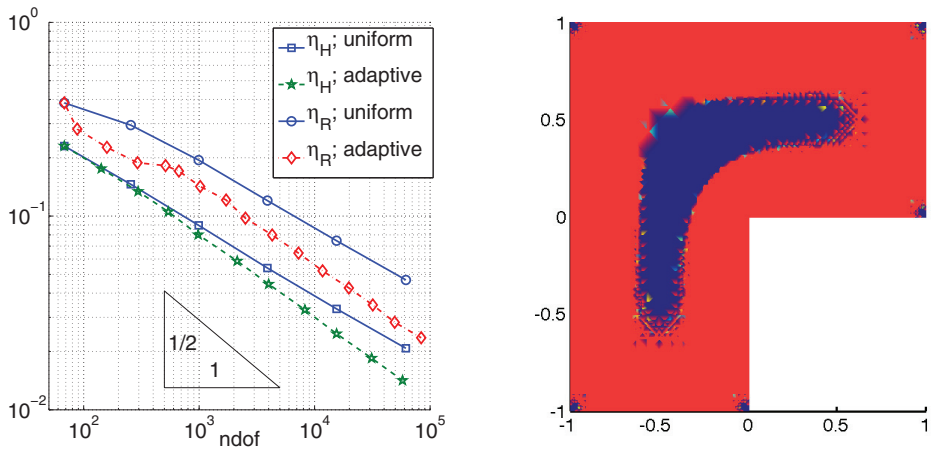
FIG. 6.14. *Convergence history η_R for adaptive and uniform refinement on all benchmark domains.*

(a) Convergence history for uniform and adaptive refinement for the error estimators.

(b) Volume fraction for the L-shaped domain.

FIG. 6.15. *L-shaped domain for a material distribution of $\xi = 0.8$.*

The error estimators and square root of extrapolated energy errors $\delta_\ell^{1/2} := |E(\sigma_{\varepsilon h})$ $-E_A|^{1/2}$ and $\delta_\ell^{*1/2} := |E^*(\sigma_{\varepsilon h}) - E_A^*|^{1/2}$ are plotted in a double logarithmic scaling depending on the ndof.

With the L-shaped domain and adaptive refinement the rate of convergence compared to uniform refinement is improved significantly. Apparently, the area $\{x \in \Omega \mid t_1 < |\nabla u_{\varepsilon h}(x)| < t_2\}$, where both materials are present, seems to be very small.

If the parameter ξ, which influences the volume fraction of each material, is chosen in a way such that the contact zone is just a boundary, i.e., there is no subdomain where both materials are present, the error estimators show optimal convergence; cf. Figure 6.15 for the L-shaped domain and $\xi = 0.8$.

REFERENCES

[1] D. Braess, *Finite Elements: Theory, Fast Solvers, and Applications in Solid Mechanics*, Cambridge University Press, Cambridge, UK, 1996.

[2] F. Brezzi and M. Fortin, *Mixed and Hybrid Finite Element Methods*, Springer-Verlag, New York, 1991.

[3] C. Carstensen, *Numerical analysis of microstructure*, in Theory and Numerics of Differential Equations (Durham, 2000), J. P. Coleman, J. F. Blowey, and A. W. Craig, eds., Universitext, Springer-Verlag, Berlin, 2001, pp. 59–126.

[4] C. Carstensen and S. Bartels, *A convergent adaptive finite element method for an optimal design problem*, Numer. Math., 108 (2007), pp. 359–385.

[5] C. Carstensen and R. H. W. Hoppe, *Error reduction and convergence for an adaptive mixed finite element method*, Math. Comp., 75 (2006), pp. 1033–1042.

[6] C. Carstensen and S. Müller, *Local stress regularity in scalar nonconvex variational problems*, SIAM J. Math. Anal., 34 (2002), pp. 495–509.

[7] C. Carstensen and P. Plecháč, *Numerical solution of the scalar double-well problem allowing microstructure*, Math. Comp., 66 (1997), pp. 997–1026.

[8] C. Carstensen and A. Prohl, *Numerical analysis of relaxed micromagnetics by penalised finite elements*, Numer. Math., 90 (2001), pp. 65–99.

[9] M. Chipot, *Elements of Nonlinear Analysis*, Birkhäuser Adv. Texts Basler Lehrbücher, Birkhäuser Verlag, Basel, Boston, Berlin, 2000.

[10] P. Clément, *Approximations by finite element functions using local regularization*, Rev. Française Automat. Informat. Recherche Opérationnelle Sér. Rouge Anal. Numer., 9 (1975), pp. 77–84.

[11] D. A. French, *On the convergence of finite-element approximations of a relaxed variational problem*, SIAM J. Numer. Anal., 27 (1990), pp. 419–436.

[12] V. Girault and P.-A. Raviart, *Finite Element Methods for Navier-Stokes Equations*, Springer Ser. Comput. Math. 5, Springer-Verlag, Berlin, Heidelberg, New York, 1986.

[13] R. Glowinski, *Numerical Methods for Nonlinear Variational Problems*, Springer-Verlag, New York, 1984.

[14] R. Glowinski, J.-L. Lions, and R. Trémolières, *Numerical Analysis of Variational Inequalities*, Stud. Math. Appl. 8, North–Holland, Amsterdam, New York, 1981.

[15] W. Han, *A Posteriori Error Analysis via Duality Theory: With Applications in Modeling and Numerical Approximations*, Adv. Mech. Math. 8, Springer-Verlag, New York, 2005.

[16] J.-B. Hiriart-Urruty and C. Lemaréchal, *Fundamentals of Convex Analysis*, Grundlehren Text Ed., Springer-Verlag, Berlin, 2001.

[17] B. Kawohl, *Rearrangements and Convexity of Level Sets in PDE*, Lecture Notes in Math. 1150, Springer-Verlag, Berlin, Heidelberg, 1985.

[18] B. Kawohl, J. Stara, and G. Wittum, *Analysis and numerical studies of a problem of shape design*, Arch. Rational Mech. Anal., 114 (1991), pp. 349–363.

[19] R. Kohn and G. Strang, *Optimal design and relaxation of variational problems* I, Comm. Pure Appl. Math., 39 (1986), pp. 113–137.

[20] R. Kohn and G. Strang, *Optimal design and relaxation of variational problems* II, Comm. Pure Appl. Math., 39 (1986), pp. 139–182.

[21] R. Kohn and G. Strang, *Optimal design and relaxation of variational problems* III, Comm. Pure Appl. Math., 39 (1986), pp. 353–377.

[22] F. Murat and L. Tartar, *Calcul des variations et homogénéisation*, in Les méthodes de l'homogénéisation: Théorie et applications en physique, D. Bergmann, J. Lions, G. Papanicolaou, F. Murat, L. Tartar, and E. Sanchez-Palencia, eds., Collect. Dir. Études Rech. Elec. France 57, Eyrolles, Paris, 1985, pp. 319–369.

[23] F. Murat and L. Tartar, *Optimality conditions and homogenization*, in Nonlinear Variational Problems, A. Marino, L. Modica, S. Spagnolo, and M. Degiovanni, eds., Res. Notes in Math. 127, Pitman, Boston, MA, 1985, pp. 1–8.

[24] A. Prohl, *Computational Micromagnetism*, Teubner, Stuttgart, Leipzig, Wiesbaden, 2001.

[25] E. Zeidler, *Nonlinear Functional Analysis and Its Applications* III.: *Variational Methods and Optimization*, Springer-Verlag, New York, 1985.